Journal of Transport & Health 38 (2024) 101829

Contents lists available at ScienceDirect

Journal of Transport & Health

journal homepage: www.elsevier.com/locate/jth

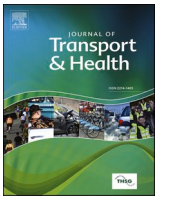

A quantitative microbial risk assessment approach to estimate exposure to SARS-CoV-2 on a bus

Andrew M. Bate [a,b,1,*], Daniel Miller [c], Marco-Felipe King [a], Katy-Anne Moseley [a], Jingsi Xu [d], Ian Hall [d], Martín López-García [b,2], Simon T. Parker [c,2], Catherine J. Noakes [a,2]

[a] School of Civil Engineering, University of Leeds, Leeds, UK
[b] School of Mathematics, University of Leeds, Leeds, UK
[c] Defence Science and Technology Laboratory, Salisbury, UK
[d] Department of Mathematics, University of Manchester, Manchester, UK

ARTICLE INFO

Keywords:
Modelling
Prevalence
Masks
Airborne
Fomite
Close-range

ABSTRACT

Introduction: We adapt and extend the Transmission of Virus in Carriages (TVC) model, a Quantitative Microbial Risk Assessment (QMRA) computational model originally developed to estimate exposure risk to SARS-CoV-2 in a subway carriage, to estimate exposure risk on a bus. The aim is to analyse the relative importance of different behavioural and environmental factors influencing exposure in this public transport setting, especially exposure to large doses when considering viral load variability between infectious passengers.

Methods: The QMRA model considers individual exposure during a bus journey through three routes: close-range exposure to aerosols and droplets due to being at close proximity (<2m) of an infected passenger, long-range airborne exposure at long distances (>2m), and transmission via contaminated surfaces (fomite route).

Results: Model predictions show that disease prevalence and bus loading levels have a major impact both on the likelihood of exposure and probability of receiving a large dose. Mask wearing is predicted to greatly reduce the magnitude of doses received, especially from close-range exposure. Assumptions around viral load also have a major impact on doses received, with large long-range airborne doses only occurring under very wide viral load distributions. Doses are not uniform around the bus, with close-range dose being generally more likely in the middle of the bus and fomite doses depending on the types of available surfaces around passengers' seated/standing positions. Surface contamination is predicted to be greatest on traversal poles that may be touched by many passengers while boarding and alighting.

Conclusions: These model predictions have implications on the effectiveness of various mitigations to SARS-CoV-2 transmission on buses.

* Corresponding author.
E-mail address: a.m.bate@leeds.ac.uk (A.M. Bate).
[1] Joint first authorship.
[2] Joint senior authorship.

https://doi.org/10.1016/j.jth.2024.101829
Received 14 November 2023; Received in revised form 2 May 2024; Accepted 13 May 2024
Available online 15 June 2024

1. Introduction

The COVID-19 pandemic has had a profound impact on society, with severe economic and societal ramifications worldwide. The SARS-CoV-2 virus is spread through respiratory droplets and aerosols generated during activities such as breathing, talking, and coughing. The ability to quantify exposure in different situations is crucial to introducing mitigation strategies and reducing infection risk. Close-range exposure to droplets and aerosols, through inhalation or direct deposition onto mucous membranes, coupled with long-range airborne exposure via small aerosols appears to be the primary mode of transmission in indoor settings (Azimi et al., 2021; Miller et al., 2021). However, transmission is also possible through contact with contaminated surfaces and subsequent touching of mucous membranes, namely: fomite transmission (Pitol and Julian, 2021; Miller et al., 2022). The relative significance of these various transmission routes is likely to be environment-specific, and it is still an ongoing question in particular in public transport settings. Known risk factors include close proximity to infected individuals, prolonged exposure, activities that generate more aerosols, and poorly ventilated enclosed spaces.

COVID-19 incidence and mortality amongst public transport workers was high during the first wave in the UK (Windsor-Shellard and Butt, 2020) and continued to be so in the USA (Heinzerling, 2022; Tomasi et al., 2021; Cummings et al., 2022). While multiple systematic factors such as ethnicity, socio-economic background and living arrangements are likely to be important (Goldblatt and Morrison, 2020), the high rates raised important questions for transmission in public transport. Studies have found viral RNA on surfaces within buses (Moreno et al., 2021; Caggiano et al., 2021; Guadalupe et al., 2022; Aranega-Bou et al., 2024), trains (Caggiano et al., 2021; Aranega-Bou et al., 2024) and metro trains (Moreno et al., 2021). While RNA on surfaces does not necessarily indicate the presence of live virus at the time of sampling, it can be a proxy for the level of contamination on different types of surfaces in a given vehicle.

Identifiable transmission of SARS-CoV-2 on public transport is tenuous due to extraneous confounding factors such as the difficulty in tracing passengers, especially on urban routes. However, some studies including analysis of an outbreak on a bus in China suggest that, where it occurs, one of the dominant factors lies around insufficient ventilation (Cheng et al., 2022). Journey duration may also be important with a study on long distance rail travel on mainland China showing a positive correlation between infection rate and prior travel by train during holiday seasons, although the exact moment(s) of infection were indeterminable (Hu et al., 2021). Schöll et al. (2024) found using epidemiological analysis of a phylogenetically unique strain that bus-riding children at a school in Germany had a four times higher attack rate than other children at that school. In contrast, a study on an independent school bus service in Virginia (Ramirez et al., 2021) where universal masking and basic ventilation techniques were mandatory, found no evidence of transmission linked to school bus transportation, suggesting the interventions had a mitigating effect. Additionally, transmission events may occur when individuals are travelling together, such as in family groups or with coworkers, which can extend the duration and nature of close contact (and make identifying where transmission occurred difficult). Understanding the factors that influence transmission risk is crucial for implementing and managing effective mitigation strategies, particularly in urban transportation systems which carry large numbers of people and where social distancing can be challenging.

Quantitative Microbial Risk Assessment (QMRA) is a modelling tool for evaluating the factors that influence the transmission of pathogens. This method uses probabilistic approaches to estimate exposure to pathogens through various routes to calculate individual infection risk. These models include the physical mechanisms of transmission, which allows them to consider the impact of environmental and behavioral interventions at a local level. Most of the recently developed QMRA models for SARS-CoV-2 focus on long range airborne transmission, omitting doses received from touching contaminated surfaces or being within close proximity to an infectious individual. In contrast, Computational Fluid Dynamics (CFD) models have been used to explore local variations in exposure due to the emission and dynamics of droplets from human respiratory activities in public transport settings (Wang et al., 2022), including car cabins (Mathai et al., 2021; Arpino et al., 2022; Sarhan et al., 2022), buses (Cheng et al., 2022; Yang et al., 2020; Duan et al., 2021; Ho and Binns, 2021; Mesgarpour et al., 2021; Ooi et al., 2021; Yao and Liu, 2021), trains (Zhang and Li, 2012; Yang et al., 2018; de Kreij et al., 2022) and airplanes (Gupta et al., 2011; Talaat et al., 2021). Simplified methodologies which typically rely on the assumption of well-mixed air, based on modified versions of the Wells-Riley model, have also been exploited to estimate infection risk of SARS-CoV-2 in public transport settings (Cummings et al., 2024; Mei et al., 2022; Chen et al., 2021a; Wang et al., 2021; Shen et al., 2021; Dai and Zhao, 2020), and to quantify the impact of possible mitigations. Transmission via the fomite route has typically received less attention. However, mathematical models have been proposed (King et al., 2020; Wilson et al., 2020; Julian et al., 2009), typically calibrated via experimental data in the laboratory for different pathogens and surfaces and under different humidity-temperature conditions (Walker et al., 2022; Zhao et al., 2019), to estimate the amount of pathogen on hands and surfaces after hand-surface contacts. These have been recently implemented to estimate fomite transmission risks in different settings (King et al., 2022; Pitol and Julian, 2021). There have been few attempts (Azimi et al., 2021; Lei et al., 2018; Jones, 2020) to account for all transmission routes simultaneously when assessing exposure in different scenarios, so that the relative importance of different transmission routes can be quantified depending on the environment.

More recently, a multi-route QMRA model was proposed (Transmission of Virus in Carriages - TVC, Miller et al., 2022) to quantify the main behavioural and environmental factors influencing exposure to SARS-CoV-2 in a subway carriage. This study identified the prevalence of infection in the passenger community, as well as the loading level (i.e. passenger density) within the carriage, as the factors having the strongest impact on individual exposure risk, and the close-range route as the dominant route leading to exposure in this setting. Particular limitations of the TVC model were that the specific locations of individuals and surfaces within the carriage at any given time were not tracked, and that individuals standing versus seating were not distinguished, which may be less appropriate for other public transport settings such as buses. Additional limitations included the consideration of a fixed viral load among infected individuals, not accounting for population heterogeneity in infectiousness, that masks were assumed to block 100% of large droplets,

and that passengers never sanitised their hands during journeys.

In this work, we extend the TVC methodology in Miller et al. (2022) to address these and other limitations while studying a different public transport setting: a bus. In Section 2, we outline the main methodological aspects of the adapted and extended QMRA model for a bus setting, with special focus on additional functionalities. Tracking individuals' locations during their journey allows one to study mitigations such as social distancing. It also allows for the analysis of risk factors related to particular spatial locations within the bus, such as the risk posed by certain seats and contaminated surfaces. In Section 3, our numerical results explore the impact of the different behavioural (mask wearing, bus route and loading patterns, hand hygiene, seating behaviours) and environmental (infection prevalence, viral load of infected passengers or ventilation) factors on exposure risk. Concluding remarks are provided in Section 4.

2. Methodology

The model in this paper extends the agent-based modelling methodology in Miller et al. (2022) to estimate exposure to SARS-CoV-2 on a bus journey. This model draws on a pre-pandemic model for transmission of viruses on aircraft (Lei et al., 2018), and also shares some characteristics with a model for COVID-19 transmission on a cruise ship (Azimi et al., 2021). The model considers the mechanistic routes of exposure together with the specific details of the transport environment and journey parameters. In this Section, we review key assumptions and major differences with respect to Miller et al. (2022), while the bulk of the details can be found in the Supplementary Material.

Like Miller et al. (2022) and Lei et al. (2018), we assume that passengers are exposed to SARS-CoV-2 via three different pathways: (long-range) airborne, close-range airborne, and fomite. We assume that each passenger has a probability of being infected (henceforth "prevalence", set to 1% as default but we will consider alternate values based on the data within Office for National Statistics, 2024), and that all virus ultimately comes from the respiratory fluid of infected passengers that is emitted by coughing (using the droplet distribution from Duguid, 1946), and such fluid that has been transferred onto the infected passenger's hands prior to boarding. Long-range airborne (henceforth, "airborne dose") is formed from small droplets (less than 20 μm in initial, wet, diameter) that are exhaled from infected passengers occasionally coughing. These droplets are assumed to instantly aerosolise, as in Wells-Riley models such as Cummings et al. (2024); Chen et al. (2021a), and spread evenly across the entire volume of the bus (minus the driver's cabin, who we do not model). These droplets are also assumed to be ventilated out of the bus (and replaced by fresh air) at a rate that is equivalent to 6 air changes per hour, henceforth "ACH", which is consistent with ventilation rates measured by Ou et al. (2022), with the balance between emissions and losses (ventilation, deposition and inactivation) dictating the airborne concentration. The long-range airborne exposure from these aerosols occurs from inhalation and from deposition onto mucosal membranes (eyes, nose and mouth). For an overview of the assumed SARS-CoV-2 exposure routes for passengers we refer the reader to (Miller et al., 2022, Fig. 1), where the same approach was followed.

Individual passengers who, at any given time, are at close proximity (within $2m$) of an infected passenger, receive a close-range airborne dose (henceforth, "close dose"). This close dose represents the inhalation and direct deposition of large droplets onto mucosal membranes of individuals within $2m$ of an infected passenger, and a four-fold increase of inhalation and membrane deposition of small aerosols when the passenger is within $1m$ of an infected passenger due to higher local concentrations (Miller et al., 2022, Fig. 1).

Lastly, to model fomites we consider the transfer of viral contamination from surfaces to the hands and from the hands to the mucosal membranes. Whenever a passenger touches their mucosal membranes with their contaminated hands, there is a transfer of some virus from their hands to the mucosal membranes. We assume passengers touch their face while onboard and for some time after

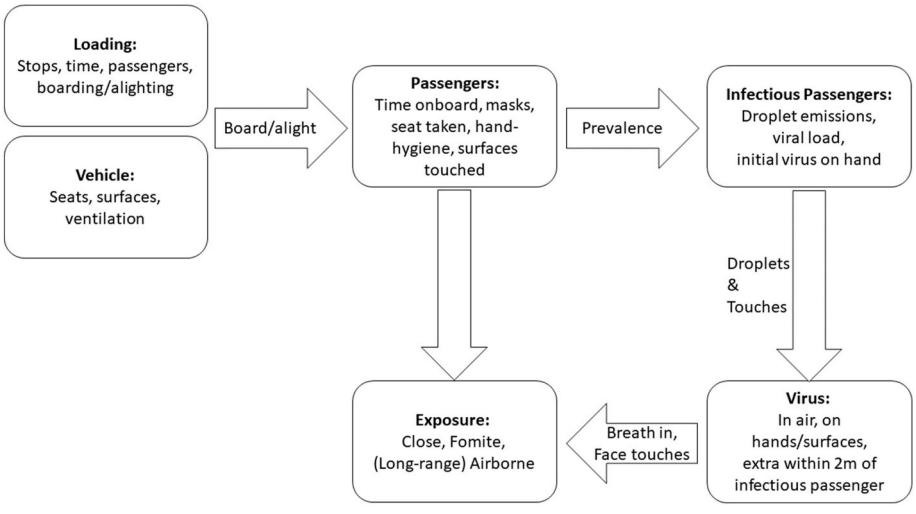

Fig. 1. A flow diagram summarising the key processes behind each simulation of the QMRA model, used to estimate the exposure to SARS-CoV-2 for each passenger during their bus journey.

alighting. The accumulation of these transfers from hand to face form the passenger's "fomite dose". Hands can get contaminated by touching contaminated surfaces, where there is a transfer of virus to and from hands governed by transfer efficiencies, the contact area and viral concentrations on hands and surfaces. Only infected passengers are assumed to have contaminated hands before boarding, with the amount depending on their viral load and the amount of fluid deposited on their hand; see Supplementary Material for details. Virus on hands and surfaces decays over time due to loss of infectivity (Harbourt et al., 2020; Matson et al., 2020). For simplicity, we assume that passengers perform all of their touches to surfaces and membranes using a single hand.

A flow diagram summarising the key processes of the QMRA model is provided in Fig. 1. There are several key differences between the model here and that in Miller et al. (2022). We model a single-decker bus with the seat and surface arrangement of the Wrightbus Streetlite 11.5*m* Door Forward - Euro 6. This bus has 1 door, 45 seats and a capacity of 72 passengers (Personal Communication with UK public transport operator, see also the Wrightbus Streetlite entry at Wikipedia (2024)); see Fig. 2(a). Unlike Miller et al. (2022), we have explicit seat locations and thus follow passenger locations, which surfaces they can interact with, and whether they are within 1 or 2 m of an infected passenger (which can lead to close-range exposure). Additionally, we consider four (4) different types of surfaces within the bus (traversal poles, seat handrails, horizontal half-poles and stop buttons). Each stop button is considered a single surface that is pressed by a fingertip, whereas all other surfaces are split into smaller, approximately hand-sized "subsurfaces' such that passengers touching these surfaces touch one subsurface at random. This results in the potential viral transfer from hand-subsurface contacts (Miller et al., 2022).

We assume the bus follows one of two (2) set routes; the *Urban* route that has 60 stops that are a minute apart, and the *Rural* route with 30 stops that are 3 min apart. These routes are inspired by the clock-face timetabling and time/distance between stops we observed in UK for a variety of urban and rural routes, but are not based on any specific bus route. We also assume three different boarding-alighting patterns based on how busy the journey is, *Half Seat*, *Full Seat* and *Full Stand*, which have a peak loading of 23, 45 and 72 passengers, respectively. Each of these loading-route patterns start and end with an empty bus, and reach peak loading some time mid-journey (Fig. 2(b)). When a passenger boards, they select an available seat (or standing location if no seats are available) at random (see Supplementary Material for other seat selection algorithms).

Unlike Miller et al. (2022), we consider an infected passenger's viral load (i.e. the viral concentration within their respiratory fluid, denoted ω), as a parameter within the model which is sampled from a (log)-Weibull distribution (Chen et al., 2021b). We also compare our results here with the fixed viral load assumption from Miller et al. (2022) (which is the 87.7th percentile of the Weibull distribution), to study the impact of considering heterogeneity in viral load across the infectious passengers' population.

The percentage of passengers wearing masks and the different types of masks worn is based on observational data collected by several UK bus operators around February–March 2022 (Confederation of Passenger Transport, Personal communication), where approximately 30% of passengers wore masks, with mask type split approximately equally between fabric and surgical-type masks, with a small minority wearing FFP2 masks (47.5%, 47.5% and 5%, respectively). Masks have an impact on the amount of droplets and aerosols that the individual exhales/inhales as well as their face-touching behaviour. The efficacy of all masks is considered to be high (but not perfect) for large droplets and moderate-to-high for smaller droplets (Aydin et al. (2020); Bandiera et al. (2020); Blachere et al. (2022); Lindsley et al. (2021), see Supplementary Material, Table 2) on both inhalation and exhalation.

Passengers are assumed to touch several surfaces during their journey. Almost all seats and standing positions have a 'positional' surface (normally a seat handrail or horizontal half-pole) that passengers touch occasionally during their time onboard. Additionally, during boarding and alighting, passengers touch a number of traversal surfaces based on how far down the bus they travel, as well as touching the positional surface of their seat (and the neighbouring aisle seat if they have a window seat). Stop buttons can also be touched at alighting by one or more alighting passengers. Each time a surface is touched, a single subsurface is touched at random. In the results, we explore the impact of sanitising hands. In particular, we consider (but not as default) the application of hand-sanitiser after boarding and/or after alighting. Applying hand-sanitiser reduces the viral concentration on hands by 95.5% (Mbithi et al., 1993).

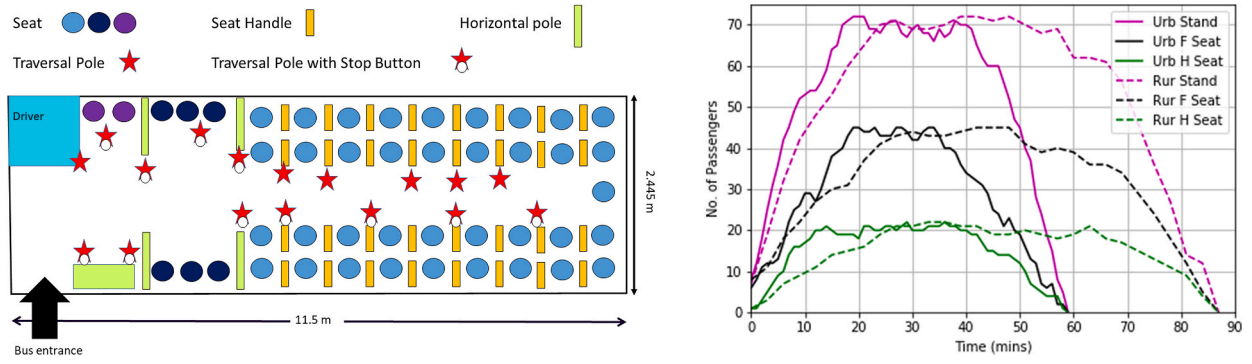

Fig. 2. (a, left) Sketch of the bus and **(b, right)** number of passengers on board over time for different loading levels and route type. In (a), large coloured circles represent available seats (blue are front facing, dark blue are folding side-facing and purple are elevated side-facing). Red stars represent traversal poles with/without stop buttons. These stop buttons are represented by small white circles attached to the star (traversal pole). Orange, shorter rectangles represent seat handrails and light green, longer rectangles represent horizontal poles.

3. Results

We examine a default set of numerous parameter values that are listed in the Supplementary Material. The main aim is to analyse the factors that affect exposure on a bus and the effects of different mitigations. Default and alternative values considered for a subset of key parameters are shown in Table 1. The rationale for selecting these parameters is indicated above in the methodology, with the alternative values selected based on ranges that were observed during different periods of the pandemic (e.g. prevalence, mask wearing) or feasible technical ventilation rates (Querol et al., 2022). We see these parameters as potentially important to exposure and can vary over time, location or by influence of policy decision. All doses are measured with respect to Plaque Forming Units (PFU).

3.1. Single journey simulation

To demonstrate how the model works and to get an understanding of the results it generates, we first look at the airborne, close and fomite doses received by passengers, and the estimated contamination of surfaces, from a single journey simulation (Fig. 3). The default "Urban Full Seat" loading-route scenario has all seats occupied at peak loading and 87 passengers travelling in total, with many seats being occupied by multiple passengers during the journey. There are 2 maskless infected passengers in this simulation. The first infected passenger sits in the back row for 46 min (boards at stop 7 and alights at stop 53) and has a very high viral load ($\omega = 1.96 \cdot 10^{15}\ PFU \cdot m^{-3}$, corresponding to the 99.5th percentile). The second infected passenger sits in the second from front row for only 7 min (boards at stop 15 and alights at stop 22) and has a moderate viral load ($\omega = 2.3 \cdot 10^{10}\ PFU \cdot m^{-3}$, around the 53rd percentile).

In this simulation only one passenger avoids receiving an airborne dose (Fig. 3(a)); this passenger alights at stop 5, which is before the first infected passenger boards the bus. This first infected passenger dominates the emissions of airborne virus due to their high viral load and presence across most of the journey. 33 passengers (out of 85 susceptible passengers) receive a non-zero close dose (Fig. 3(b)). One can observe many reds (within 1–2m) and deep reds (within 1m) around the infected passenger in the back row, whereas there are more blues (within 1m) and dark blues (within 1–2m) for passengers around the infected passenger nearer the front. This difference of many orders of magnitude is a consequence of the big difference in viral loads between infectious passengers and to a lesser degree the times onboard for both of these passengers.

Most passengers receive a non-zero fomite dose (68 out of 85 susceptible passengers), however these passengers are scattered across all areas of the bus (Fig. 3(c)). It appears that passengers nearer the front and passengers that alight early enough for their seat to be filled by another passenger after them are more likely to avoid receiving a fomite dose (as more surfaces will become contaminated over time). The size of the dose varies significantly and has no clear pattern, with all colours including reds, yellows and blues spread across the bus. Although patterns for fomite dose might be relatively weak due to the stochastic effect of both touching a surface and touching mucous membranes, there is a clearer trend for concentrations on surfaces (Fig. 3(d)). The highest contaminated surfaces are observed to be those that were touched by the back row infected passenger, which are the seat handrails associated to their seat and neighbouring aisle seat (which they touch when boarding and alighting), and the stop button at the back of the bus which they touch when alighting. Other surfaces predicted to be highly contaminated are the traversal poles, ranging from orange to deep red. Stop buttons have a wide range of contamination, including one that is uncontaminated by the front door (stop buttons are considerably smaller than other surfaces so the same number of virus leads to much higher concentrations). Many seat handrails are contaminated, but 13 out of 32 remain uncontaminated; with seat handrails seeming to be more likely to be contaminated in pairs. This makes sense as someone with contaminated hands using a window seat is assumed to touch both the window seat's and aisle seat's seat handrails when boarding and alighting.

Lastly, comparing the non-zero doses, the airborne dose has a relatively limited range, with doses ranging from around 0.055 PFU to 45 PFU, whereas close doses range from around 0.0007 PFU to 11, 500 PFU and fomite doses range from around $6.5 \cdot 10^{-5}\ PFU$ to 26, 600 PFU.

3.2. Exposure routes and impact of viral load heterogeneity

In this section, we consider results from 1000 stochastic journey simulations to explore the distribution of airborne, close and fomite doses received by passengers under default parameters in Table 1 (which includes a wide log-Weibull viral load from Chen et al. (2021b)), and compare these results with 1000 simulations where each infected passenger has the same, relatively large, fixed viral

Table 1
Parameters of interest and their values.

Parameter/option	Default	Alternatives
Viral Load	(log)-Weibull Distributed	Fixed Value (Miller et al., 2022)
Prevalence	1%	0.1%, 0.2%, 0.5%, 2%, 5%
Loading	Full Seat (peak 45, total 87)	Half Seat (peak 22, total 43); Full Stand (peak 72, total 160)
Route	Urban (60 stops, 59 min)	Rural (30 stops, 87 min)
Mask-wearing	30%	0%, 50%, 70%, 100%
Fresh-flow rate	6 ACH	1.5 ACH, 3 ACH, 12 ACH, 24 ACH
Hand-sanitising	None	Boarding only, Alighting only, Both Boarding and Alighting

Table 2
Summary statistics of doses for heterogeneous and fixed viral load (VL); see Fig. 4. Geo. Mean is the geometric mean of all non-zero doses, which is less sensitive to outliers than the arithmetic mean. NZ Dose stands for the percentage of non-zero doses. % > 7PFU corresponds to the percentage of doses larger than 7 PFU. Note that as total dose for each passenger is the sum of their airborne, close and fomite doses, the arithmetic mean of the total dose will be the sum of the mean of airborne, close and fomite doses; this property does not apply to other statistics like medians, quantiles, (non-zero) geometric means and proportion of large doses.

	Arith. Mean	NZ Dose	Geo. Mean	Median	75%ile	95%ile	Maximum	% >7PFU
Heterogeneous								
Air	$9.012 \cdot 10^{-2}$	49.7%	$5.366 \cdot 10^{-5}$	0	$5.789 \cdot 10^{-5}$	$2.953 \cdot 10^{-2}$	$6.871 \cdot 10^{1}$	0.33%
Close	$4.172 \cdot 10^{0}$	14.9%	$3.798 \cdot 10^{-3}$	0	0	$3.749 \cdot 10^{-2}$	$1.190 \cdot 10^{4}$	1.04%
Fomite	$1.621 \cdot 10^{1}$	31.3%	$2.896 \cdot 10^{-4}$	0	$7.275 \cdot 10^{-7}$	$1.389 \cdot 10^{-1}$	$1.534 \cdot 10^{5}$	1.51%
Total	$2.048 \cdot 10^{1}$	49.7%	$7.486 \cdot 10^{-4}$	0	$7.543 \cdot 10^{-4}$	$9.683 \cdot 10^{-1}$	$1.534 \cdot 10^{5}$	2.53%
Fixed VL								
Air	$9.560 \cdot 10^{-3}$	49.8%	$7.123 \cdot 10^{-3}$	0	$9.915 \cdot 10^{-3}$	$4.936 \cdot 10^{-2}$	$4.658 \cdot 10^{-1}$	0.00%
Close	$4.056 \cdot 10^{-1}$	14.8%	$7.349 \cdot 10^{-1}$	0	0	$2.519 \cdot 10^{0}$	$5.813 \cdot 10^{1}$	1.63%
Fomite	$3.167 \cdot 10^{0}$	30.9%	$4.351 \cdot 10^{-2}$	0	$8.312 \cdot 10^{-4}$	$4.760 \cdot 10^{0}$	$2.150 \cdot 10^{3}$	4.21%
Total	$3.583 \cdot 10^{0}$	49.8%	$1.219 \cdot 10^{-1}$	0	$7.850 \cdot 10^{-2}$	$8.594 \cdot 10^{0}$	$2.150 \cdot 10^{3}$	5.88%

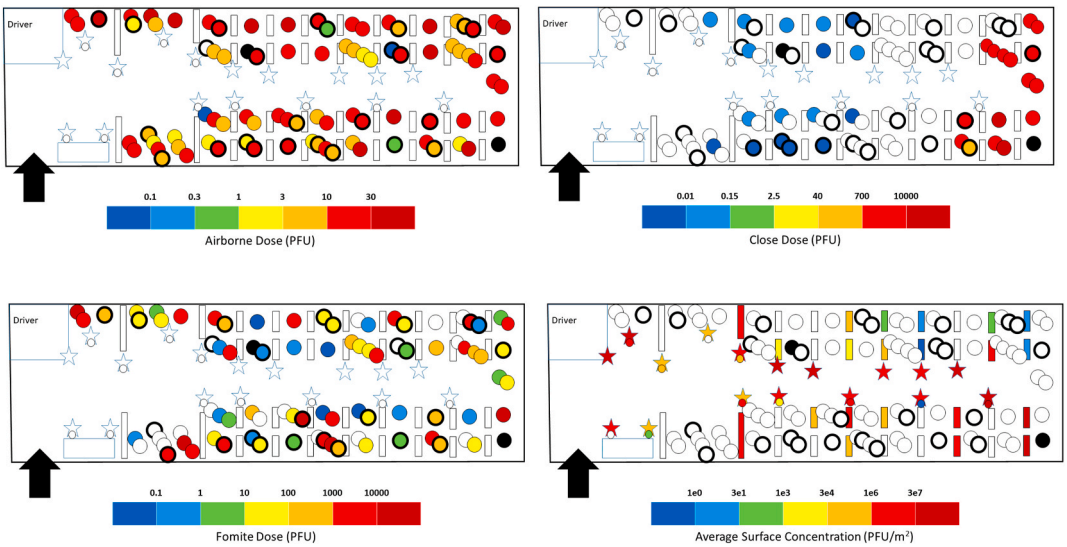

Fig. 3. Results from a selected single journey simulation for **(a, top left)** airborne dose, **(b, top right)** close dose, **(c, bottom left)** fomite dose and **(d, bottom right)** average terminal surface concentration (i.e. the mean of all subsurfaces at the last stop after the last passenger alights). Each large circle represents a passenger and where they sit, multiple passengers can occupy a seat across a trip, the more recent passengers are on top and to the bottom right. A thick outline represents that the passenger is wearing some variety of facemask. In this simulation, there are two infected passengers (in black), one in the back row and one in the second from front row; neither wears a facemask; all other passengers (85 in total) are susceptible passengers. Each subfigure has different colour-scales for doses received/surface concentration (with different units for surface concentration). The shapes (but not colours) for surfaces are same as in Fig. 2(a).

load ($\omega = 3.61 \cdot 10^{12}\ PFU \cdot m^{-3}$, 87.7th percentile) used in Miller et al. (2022).

When considering the heterogeneity in viral load across infected passengers (Fig. 4(a)), our model predicts that all doses are likely to vary by many orders of magnitude, forming wide overlapping mono-modal distributions (excluding the many zero doses). This suggests that exposure to the virus is highly stochastic, with close doses dominating airborne doses in the scenario under consideration, and fomite doses overlapping both.

The heterogeneity in viral load across infectious passengers is predicted to be the main source of stochasticity in our exposure predictions, with individual exposure risk heavily affected by the viral load of the specific infectious passenger(s) travelling during the journey. To illustrate this point, we compared our default heterogeneous viral load results with Fig. 4(b), where all infectious individuals are considered to have the same fixed viral load. With a fixed viral load, the airborne and close-range dose distributions are significantly narrower, while the fomite dose distribution still spans many orders of magnitude. This suggests that exposure through fomites is highly stochastic not just because of viral load heterogeneity, but also because its magnitude depends upon the specific sequences of contacts to subsurfaces and then to mucous membranes.

The boxplots in Fig. 4(c) confirm that fomite exposure is heavily dominated by potentially very high outliers, whereas airborne doses are more homogeneous. Close doses also contain a substantial amount of outliers, as close-range exposure can only occur by being in close proximity to an infectious passenger on a particular journey. It is important to note that while close-range exposure

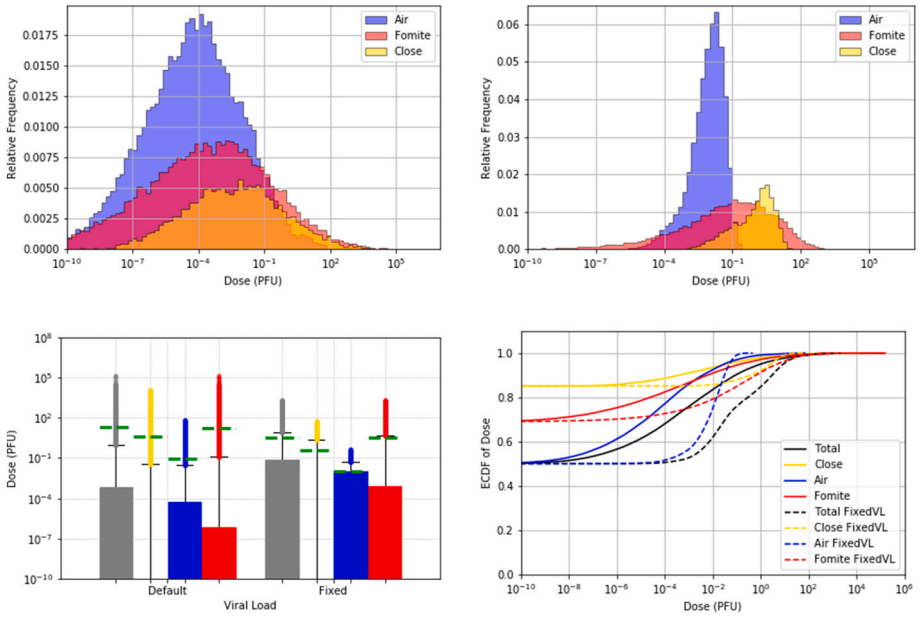

Fig. 4. The distribution of doses (close in yellow, fomite in red, airborne in blue and total in grey/black) for susceptible passengers under default parameters, represented as histograms for **(a, top left)** default heterogeneous viral load; and **(b, top right)** the fixed viral load used in Miller et al. (2022); **(c, bottom left)** boxplots of all doses (including total dose) for both default and fixed viral load; **(d, bottom right)** empirical cumulative density functions (ecdf) of all doses (including total dose) for default and fixed viral load. In (c), the whiskers represent the 95% quantile, and the green marks represent the arithmetic mean. The empirical cumulative density function of a dose X in (d) is the proportion of susceptible passengers who receive a dose less than X. Total dose is the sum of each passengers' airborne, fomite and close doses. Note that (a) and (b) have different y-axis scaling. Relevant statistics are in Table 2.

requires travelling with an infectious passenger at the same time, airborne and fomite exposure can occur even after the infectious passenger has left the bus (i.e., via contaminated air or surfaces). We discuss this in greater detail in the Supplementary Material.

Table 2 shows that a significant proportion of passengers receive no dose via any transmission route, which is why the median doses are all zero, and the empirical cumulative density function curves in Fig. 4(d) all start above 0.5. Specifically, just under 50% of passengers are predicted to receive an airborne dose - and total dose - while fomite and close doses are less likely (around 30% and 15%, respectively), but can lead to potentially higher doses. Our results for non-zero doses suggest that airborne dose is typically smaller, close dose is consistently the largest, and fomite dose is more stochastic having the largest outliers.

As a benchmark for a dose that is potentially sufficient to lead to infection, we consider doses greater than 7 PFU (the ID50 value estimated for SARS-CoV-2 by intranasal inoculation in controlled conditions (Killingley et al., 2022)). We find that about 0.3% of passengers receive an airborne dose higher than 7 PFU under this scenario, while over 1% receive a close dose, over 1.5% receive a fomite dose, and over 2.5% receive a total dose. However, it is not clear how doses received via different routes translate into infection risk, as discussed in Section 4.

If we instead consider a fixed viral load, no passenger in 1000 simulations receives an airborne dose over 7 PFU. This means that

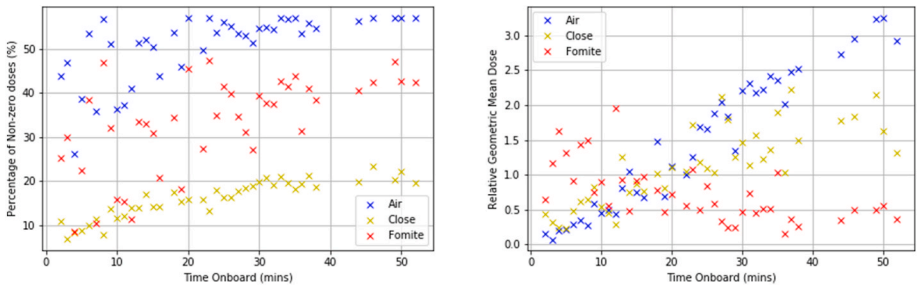

Fig. 5. (a, left) Percentage of passengers that receive a non-zero airborne, close and fomite dose by time onboard. **(b, right)** The non-zero geometric means of airborne, close and fomite dose by time onboard, relative to their respective geometric means of the total susceptible population in Table 2. The number of passengers considered for each data point is approximately 990 (from the 1000 default simulations, excluding infected passengers with 1% prevalence) multiplied by the number of passengers within the loading model 'Urban Full Seat' with that time onboard. The gaps in 'Time Onboard' occur where there are no passengers within the loading model with that time onboard.

high airborne doses are likely driven by infected passengers with very large viral loads or specific airflow patterns that are not captured in the well-mixed model assumptions. This suggests that, whilst airborne transmission from a single infectious passenger has the potential to affect more passengers, superspreading events via this route likely requires a very high viral load. For example, the single simulation in Fig. 3(a) has many passengers receiving airborne doses over 7 PFU because one passenger has a very high viral load.

3.3. Time onboard as a risk factor

We now explore how time onboard affects the doses passengers receive. In Fig. 5(a), we can see that the likelihood of receiving an airborne dose increases with time onboard, reaching over 50% for journeys lasting beyond 22 min. Close doses also become more likely as the time onboard increases, rising from around 10% for short journeys to 20% for longer journeys. The likelihood of receiving a fomite dose also appears to marginally increase with time onboard (possibly due to more face touching time), but this pattern is the weakest of the three. In Fig. 5(b), we see a clear pattern of the geometric mean of airborne doses increasing linearly with time onboard. Close doses also increase with time onboard, but with a smaller gradient and possibly flattening for longer times onboard. The magnitude of fomite doses appears to have no dependence on the duration of the passenger's time onboard.

Our results suggest that while increasing time onboard increases the likelihood of receiving an airborne and close dose for each individual passenger (and possibly the size of this dose), fomite doses cannot be avoided by reducing an individual's journey time, as they are more dependent on stochastic factors such as the number and particular sequence of surfaces touched during the journey.

3.4. Infection prevalence

Miller et al. (2022) found that infection prevalence was one of the main factors driving exposure when considering a subway carriage, so we explore this parameter here. Fig. 6 shows how increasing infection prevalence from 0.1% to 5% leads to increasing estimated doses across the passenger population, especially the frequency of non-zero doses. The first thing to note is the presence of visible quantiles as prevalence increases; for 0.1% prevalence, only the outliers are visible for close and fomite non-zero doses, whereas airborne and total doses have whiskers for the 95th percentile. This means less than 5% of passengers receive non-zero close and fomite doses. Increasing to 5% prevalence results in all doses having non-zero medians, with both lower quartiles and 5th percentile whiskers appearing for airborne and total doses.

The increase in the summary statistics such as arithmetic means and quantiles as prevalence increases can be interpreted as a reduction of the number of zero doses: increasing prevalence leads to more passengers getting a dose during their trips. However, the geometric mean of all non-zero doses also increases with prevalence, meaning the distribution of non-zero doses is getting larger with prevalence too (i.e. the histogram like Fig. 4(a) is broadly shifting to the right). We believe this is due to the possibility of susceptible passengers encountering multiple infected passengers (thus increasing their likelihood of meeting one with a high viral load) during their journey, which becomes increasingly more likely as prevalence increases. This impact is largest for the airborne dose, with nearly two orders of magnitude difference in the geometric means, with fomite over one order of magnitude and close dose less than one order of magnitude. Airborne doses are more sensitive to the prevalence as receiving airborne doses from multiple infected passengers is more likely due to the lack of proximity or surface-touch dependence. Our sample simulation (Fig. 3(a)) showed this: airborne doses are relatively high because one infected passenger has a very high viral load, whereas the other infected passenger contributed little.

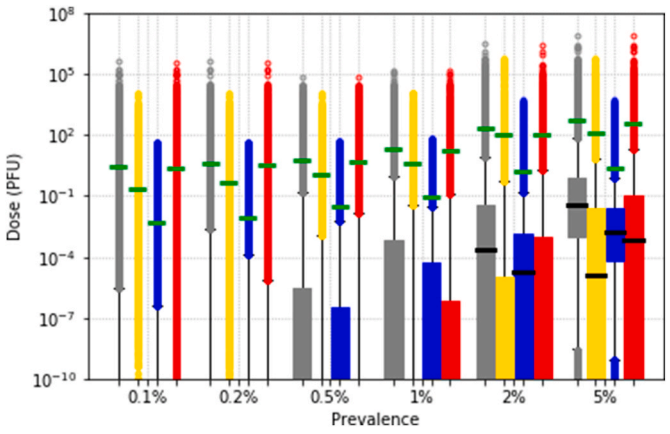

Fig. 6. Boxplot of airborne (blue), close (yellow), fomite (red) and total (grey) doses for various prevalence levels. Whiskers represent the 5th/95th percentile. Green lines represent the mean, while black lines represent median values. Summary statistics reported in Table 7 in the Supplementary Material.

3.5. Loading levels and route type

In this section, we investigate how route type (Urban vs Rural) and loading levels (Half Seat, Full Seat or Full Stand) affect exposure to the virus. Fig. 7 shows that route type has only a small impact on exposure, with the Rural route leading to slightly higher doses than the Urban route. This difference is mainly because passengers spend longer on Rural routes, consistent with results in Section 3.3.

On the other hand, loading levels have a significant impact on predicted exposure. Firstly, as passenger numbers increase (from a half-seated bus to a full-seated and full-standing bus), the likelihood of receiving any dose increases. In the full-standing scenario, only 30% of passengers avoid receiving a dose, compared to just over 50% for full-seated and over 70% for half-seated. Loading levels have a greater impact on close and fomite doses than on airborne doses. The differences in close and fomite doses between half-seated and standing models are about three orders of magnitude at the 95th percentile, with even greater differences at the upper quartile and median levels. Increasing loading levels increase the likelihood of passengers seating (or standing) in close proximity to each other and increases the potential spread of the virus across surfaces due to more hand-surface contacts.

3.6. Mask wearing as a mitigation

In this Section, we look at the impact of mask wearing on exposure, and we refer the reader to the Supplementary Material for detailed assumptions around mask filtration efficacies. Fig. 8 suggests that increasing mask frequency significantly reduces airborne and close doses. Specifically, the upper quartile dose for airborne doses decreases by more than an order of magnitude, and the 95th percentile dose decreases by about an order of magnitude. For close doses, we observe a similar trend, with a reduction of over an order of magnitude at the 95th percentile, which also applies to the highest doses. However, for fomite doses, we see a weaker pattern of decreasing dose as mask frequency increases.

When comparing 0% and 100% masking scenarios, we see a substantial decrease in maximum doses for airborne and close doses, dropping from around 85 and 13, 000 PFU to around 30 and 350 PFU, respectively. For doses over 7 PFU, we observe reductions of around 0.35%, 1.4%, and 0.5% for airborne, close, and fomite doses, respectively, when increasing mask frequency from 0% to 100%. These results suggest that increasing mask-wearing frequency is an effective measure in reducing exposure to SARS-CoV-2 on public transportation, consistent with results in Miller et al. (2022).

The impact of mask frequency on exposure is shown in Fig. 8(b). The blue solid and dashed lines represent the arithmetic and geometric means of airborne doses, respectively. Both the arithmetic and geometric means consistently decrease, resulting in a 50% reduction at 50% masking and a 75% reduction when everyone wears a mask. This is because most masks, such as surgical and fabric masks, reduce exhaled small droplets from infected passengers by approximately 50% and inhaled small droplets from susceptible passengers by approximately 50%. For close doses, the impact is even more significant, with both arithmetic and geometric means decreasing by two or more orders of magnitude. The results for fomite doses have more variability, but they settle with a 40–50% reduction at 100% masking, compared to 0% masking, as a result of masked passengers touching their membranes less frequently.

It is important to note that mask frequency does not affect the probability of receiving a dose since masks are not 100% efficient at filtering small and large droplets. Although the modelled reduction in face-touching frequency (from 11.14 to 3 touches per hour) due to wearing a mask is significant, passengers are assumed to touch their mucosal membranes unmasked for some time after alighting, which could dilute the reduction in face-touching frequency. This is especially true since these face touches include contamination picked up from surfaces while alighting.

We conducted simulations with a 75% mask frequency to explore the impact of mask type, where Fabric, Surgical, and FFP2 masks

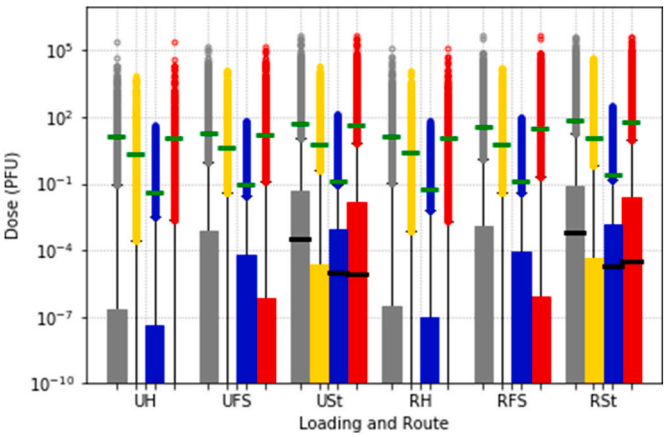

Fig. 7. Boxplots of airborne (blue), close (yellow), fomite (red) and total (grey) doses for various routes and loading intensities. Whiskers represent the 5th/95th percentile. Green lines represent the mean, while black lines represent median values. UH: Urban Half Seat, UFS: Urban Full Seat, USt: Urban Full Stand, RH: Rural Half Seat, RFS: Rural Full Seat, RSt: Rural Full Stand. Summary statistics reported in Table 8 in the Supplementary Material.

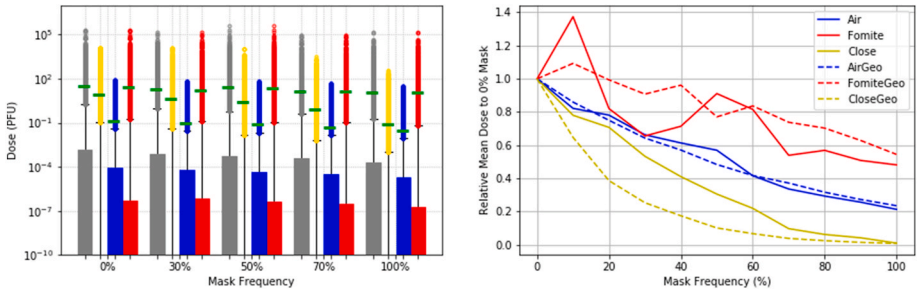

Fig. 8. (a, left) Boxplot of airborne (blue), close (yellow), fomite (red) and total (grey) doses for various proportions of passengers wearing masks. Whiskers represent the 5th/95th percentile. **(b, right)** A line graph of the various arithmetic (solid lines) and (non-zero) geometric (dashed lines) mean doses as a function of mask frequency, relative to 0% mask frequency, with mask increments of 10%. Summary statistics are in Table 9 in the Supplementary Material.

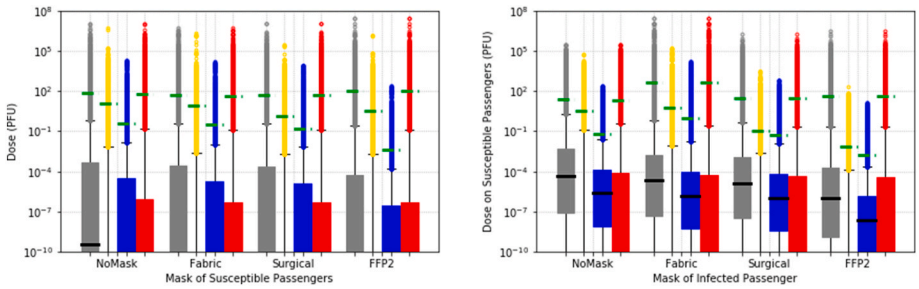

Fig. 9. Boxplots of airborne (blue), close (yellow), fomite (red) and total (grey) doses received by susceptible passengers by type of mask (or lack of mask) worn by **(a, left)** the susceptible passenger, and **(b, right)** the infected passenger. Results generated from 50,000 simulations, with default parameters except that mask frequency is 75% and that each of the 3 mask types are equally likely (i.e. 25% wear no mask, 25% wear a surgical mask, 25% wear a fabric mask and 25% wear an FFP2 mask). In (b), we only use simulations from the 50,000 that have one infected passenger on the journey (about 37.5% of simulations); of these infected passengers the top 5 viral loads are all wearing fabric masks, the top viral load being $1.5 \cdot 10^{18}$ $PFU \cdot m^{-3}$ whereas the top viral load among those not wearing a fabric mask is $5 \cdot 10^{16}$ $PFU \cdot m^{-3}$. Consequently, in (b), the arithmetic mean, maximum doses and possibly the percentage of > 7 PFU doses are skewed for the fabric mask category. Summary statistics are reported in Tables 10 and 11 in the Supplementary Material.

were equally likely. We focused on the masks worn by susceptible passengers (Fig. 9(a)) and found that there was a consistent hierarchy of mask types for all dose measures (especially airborne doses), with passengers not wearing masks (NoMask) receiving the highest doses, followed by Fabric, then Surgical, and finally FFP2 by a big margin; a hierarchy consistent with the filtration efficiencies of each mask type (Table 2, Supplementary Material). For close doses, there was less difference between mask types, but a considerable reduction compared to NoMask as all masks are effective at blocking large droplets. For fomite dose, there was no real difference between all three mask types, but a small difference between wearing a mask and NoMask for the estimated dose received by the

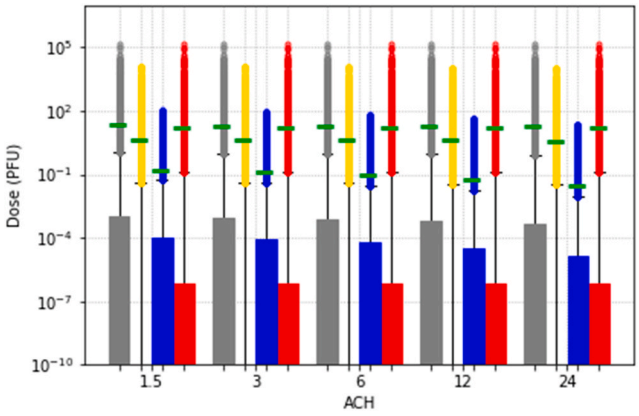

Fig. 10. Boxplots of airborne (blue), close (yellow), fomite (red) and total (grey) doses for various ventilation rates. Whiskers represent the 5th/95th percentile. Summary statistics are reported in Table 12 in Supplementary Material.

susceptible passenger, as mask-wearing affects mucosal membrane touches when worn.

Next, we focused on the consequence of the mask worn by the infected passenger on the doses received by the susceptible passengers in simulations with only one infected passenger (Fig. 9(b)). We found that all three mask types reduced close doses compared to NoMask by at least one order of magnitude, whereas for airborne doses, Fabric reduced the 95th percentile by about 39%, Surgical by 56%, and FFP2 by 99% (consistent with the small droplet filtration efficiencies in Table 2, Supplementary Material). FFP2 masks were the most effective at reducing doses, especially airborne doses, whereas the other masks still substantially reduced doses, especially close doses.

Comparing the results of susceptible and infected passengers at the 95th percentile, we found that there was not much impact on who wears the mask, except for the close doses over 7 PFU, which dropped significantly when infected passengers wore any mask. This is likely due to susceptible mask wearers experiencing a typical amount of deposition of larger droplets onto the mucosal membranes around the eyes, whereas such deposition would be greatly reduced if the exhaling infected passenger wears any mask.

3.7. Ventilation rates

Fig. 10 shows that ventilation has no impact on fomite dose and a small impact on close doses, but a significant impact on airborne doses. As ventilation increases from 1.5 ACH to 24 ACH, the airborne dose decrease by over one order of magnitude at the upper quartile level, and to around one order of magnitude at the 95th percentile. This suggests that increasing ventilation leads to a consistent decrease in airborne doses across the board. However, the effect on the total dose is rather limited, with negligible impact on the higher total doses like at the 95th percentile, but with a visible impact at the upper quartile level. This is consistent with the idea that airborne doses are typically more frequently received but smaller in this scenario. For airborne doses, increasing from 1.5 ACH to 24 ACH leads to about a 4–5 fold decrease in the maximum doses and the percentage of doses over 7 PFU. Our results thus suggest that increasing ventilation rates would have a more significant impact in reducing exposure in journeys where a highly infectious individual travels for a long time in a crowded bus. This has increased importance as it is this confluence of high viral load and long journey time on a crowded bus which is expected to produce super-spreading events.

3.8. Hand-sanitising as a mitigation

Fig. 11 shows that sanitising hands can significantly reduce the fomite dose, with a difference of almost two orders of magnitude at the 75th percentile between passengers who sanitise their hands both at boarding (when they reach their seats) and (just after) alighting; whereas at the 95th percentile, there is over one order of magnitude difference compared to no hand-sanitising. The percentage of fomite doses over 7 PFU also decreases from over 1.5% to under 0.5%. We note that while each application of hand-sanitiser is assumed to reduce hand contamination by 95.5%, the impact on exposure is different depending on when the hand-sanitising event occurs (i.e. at boarding or alighting). In particular, sanitising hands after alighting can protect the passenger from the fomite dose received from face touches after alighting, but it does not affect fomite doses received before alighting, nor the contamination of hands and surfaces within the bus. In other words, hand-sanitising after alighting is only self-protective. Conversely, sanitising hands after boarding reduces hand contamination while onboard, but it has no impact on traversal and positional touches during boarding. Hence, contamination by unsanitised hands would already spread across the bus. This boarding contamination has a disproportional impact via the traversal surfaces earlier on in the journey, allowing more time for it to be touched by other passengers and spread onto mucosal membranes and other surfaces. Additionally, after boarding, we assume that the infected passenger's positional surface will gradually become more contaminated by respiratory emissions, which hand-sanitising cannot prevent. This contamination can lead to more contamination on the recently sanitised hands through touching their positional surface while seated.

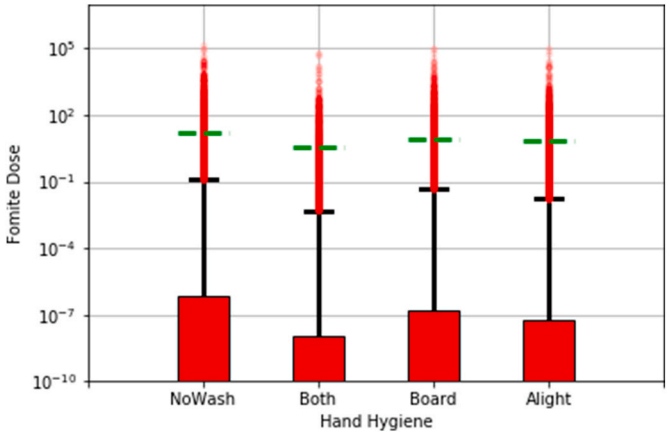

Fig. 11. Boxplots of fomite dose for different hand-sanitising scenarios (airborne and close doses are unaffected by hand-sanitising). Whiskers represent the 5th/95th percentile. Summary statistics are reported in Table 13 in Supplementary Material.

Overall, hand-sanitising after boarding can reduce surface contamination on the bus and benefit other passengers, but the effect is relatively weak. On the other hand, scenarios where the infected passenger sanitises their hands before boarding (not considered here) would likely lead to a more significant impact, preventing contamination of traversal surfaces during boarding.

3.9. Predicted contamination of surfaces

To better understand fomite exposure (and potentially the surfaces to target for cleaning), we study the predicted surface contamination levels in our simulations. Fig. 12(a) shows that seat handrails and horizontal poles are infrequently contaminated, whereas traversal poles (and to a lesser extent stop buttons) are frequently contaminated.

We next explore if there are any spatial patterns of surface contamination by focusing on the 75th and 95th percentiles of surface contamination (Fig. 12(b) and (c)). Fig. 12(b) shows a clear pattern of high concentration for traversal poles throughout the bus. The stop buttons have highest concentrations at the back of the bus with low or zero concentrations near the front, which is a consequence of stop buttons near the back serving 8 or 9 seats and those near the front serving only a few seats. For seat handrails, there is a clear pattern where only seat handrails for aisle seats receive a non-zero concentration at the 75th percentile, and that these concentrations get progressively larger as one moves towards the back of the bus (going from dark blues to greens and yellows). The aisle seat phenomena results from the aisle seat handrails being touched by passengers while boarding and alighting from the adjacent window seat, essentially doubling the number of passengers that touch the surface compared to the window seat handrails. Higher contamination as one progresses down the bus is likely the result of passengers seated near the back touching more traversal poles. For horizontal poles, we also see a split at the 75th percentile: the two half poles in front of the first row have similar concentrations to aisle seat handrails (especially those near the middle rows), whereas the two half poles nearest to the front door are both zero at the 75th percentile; the former are positional surfaces shared between two seats whereas the latter are positional surfaces for one or no seats. The results at the 95th percentile are similar to the 75th percentile (Fig. 12(c)). However, only two surfaces have zero concentration and both have no seats positions associated with them.

Overall, our results suggest that traversal poles are most likely to be contaminated and are predicted to have the highest levels of contamination at almost all quantiles. This is the result of these surfaces being touched frequently by many passengers (including infected passengers) both at boarding and alighting, whereas most other surfaces are more restrictive on who can touch them and when.

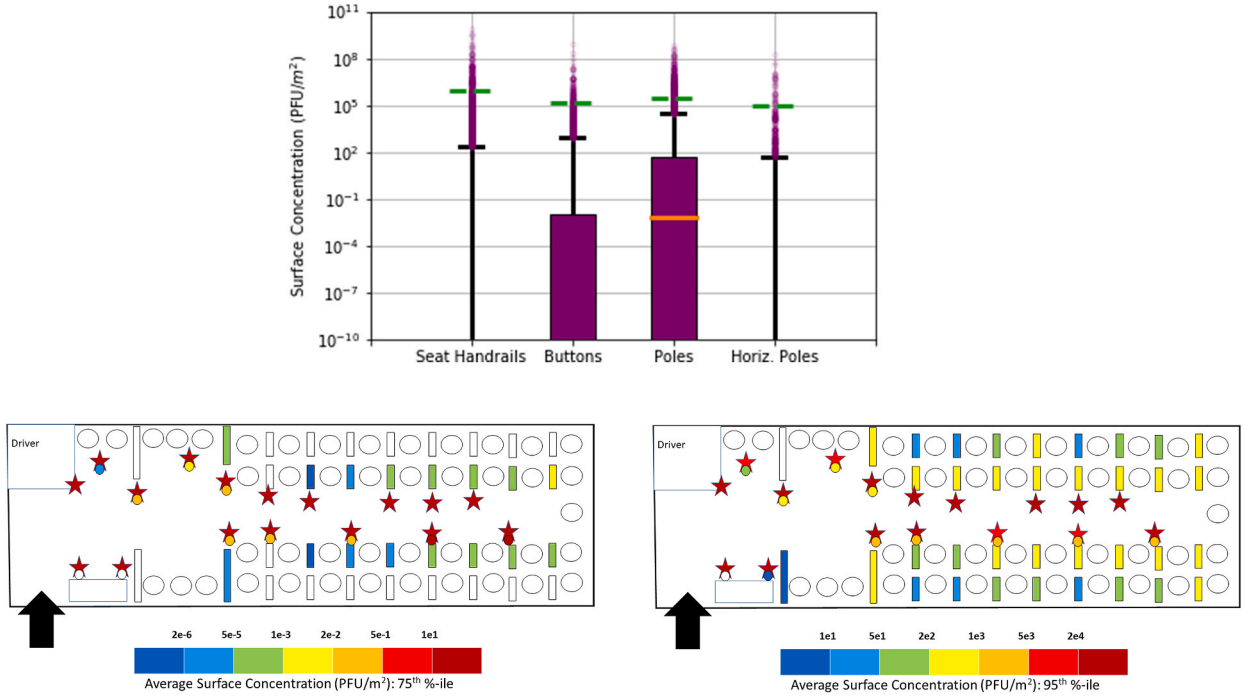

Fig. 12. Surface concentration (averaged across subsurfaces) at the end of 1000 simulations under default parameters in Table 1. **(a, top)** Boxplots by surface category. **(b, bottom left)–(c, bottom right)** Bus diagrams with surfaces colour-coded by viral concentration at the 75th and 95th percentile, respectively. Note that in (b) and (c), the colour scales are different, and that white surfaces have no predicted surface contamination at the corresponding percentile, i.e. if a 75th percentile surface is white then at least 75% of vehicles simulated have no contamination on this surface. The shapes (but not colours) for surfaces are same as in Fig. 2(a).

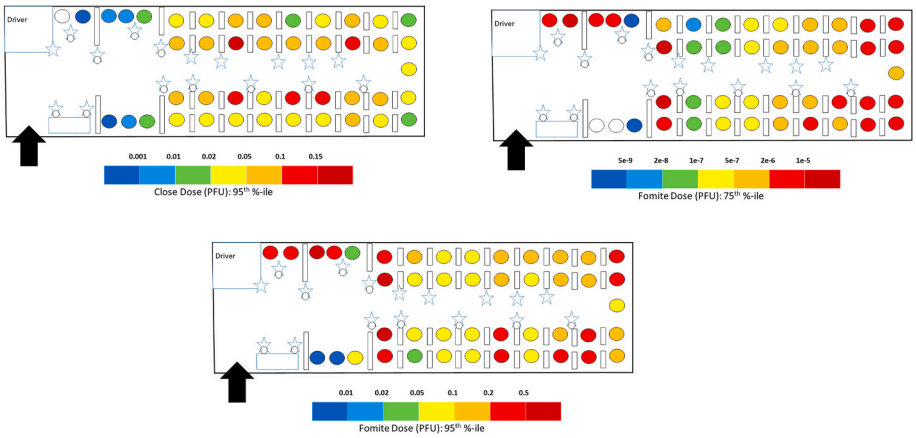

Fig. 13. Passenger doses by seat position from 1000 simulations. **(a, top left)** Close dose at 95th percentile. **(b, top right)** Fomite dose at 75th percentile. **(c, bottom)** Fomite dose at 95th percentile. In each figure, the colour scale is different. White seat positions receive no dose at that percentile. Default parameter conditions in Table 1 are used, including Full Seat Loading. The shapes (but not colours) for surfaces and seat positions are same as in Fig. 2(a).

3.10. The impact of seating position

Fig. 13 explores the doses received by passengers based on their seating positions under default conditions (such as Full Seat loading). For close doses (Fig. 13(a)), at the 95th percentile of passengers who sat each position, the lowest doses are at the front (blues and greens), where they have the fewest neighbours within 2m, with the seat directly behind the driver having less than 5% non-zero doses. The highest doses (dark reds, reds and oranges) seem to correspond to those passengers in aisle seats in middle rows, being the ones that have the most neighbours. The difference between dark red and dark blue is at least a factor of 150.

For fomite doses, we explore both the 75th and 95th percentiles (Fig. 13(b) and (c)). Seats nearer the back receive higher doses, especially for the 75th percentile where the doses vary by several orders of magnitude. This is consistent with the higher surface concentrations predicted on seat handrails nearer the back of the bus in the previous subsection. At the 75th percentile, two doorside folding seats have no dose. This suggests that seat position can have a significant impact on exposure risk, especially as these seats require few traversal touches. However, the driverside folding seats near the front receive higher doses, as they have traversal poles (which have higher surface concentrations) as positional surfaces whereas the doorside seats do not (in fact the middle doorside folding seat has no positional surface). Likewise, the front row passengers also have high fomite doses as the aisle seats have traversal poles as their positional surface, which also means that window seats touch these traversal poles when boarding and alighting. Another local effect that becomes apparent here is that the middle back seat seems to have lower fomite doses than others at the back, which makes sense as it is a seat without a positional surface.

Overall, close dose is highest (especially on number of non-zero doses) for seats with most near-neighbours (i.e. aisle seats in middle rows). For fomite, a general pattern of higher fomite doses the further to the back of the bus is seen as a result of more traversal surfaces touched; however this effect can be small compared to local issues like positional surfaces, with the highest fomite doses at seats that have traversal poles as positional surfaces.

4. Discussion

In this paper, we investigate exposure to SARS-CoV-2 during a bus journey and show through a QMRA model how exposure via three different routes: long-range airborne, close-range and fomite, can be explored. The results throughout show a high degree of variability that reflect both the virus parameters and the different human interactions in the transport environment. Similar levels of variability are seen in other QMRA studies including Jones (2020), Lei et al. (2018) and Azimi et al. (2021). Exposure distributions are analysed according to several different measures. Some of these were similar to those in Miller et al. (2022), such as arithmetic mean, median and percentage of non-zero doses. However, when accounting for variability in viral load, these measures do not sufficiently cover the shape of the exposure distribution and in particular do not place sufficient emphasis on the highest doses which may pose the highest risk for infection. As such, we also make use of the non-zero geometric mean as a central estimate less affected by outliers and the 75th and 95th percentiles to analyse the distribution of doses received by susceptible passengers in a range of scenarios.

Given the very wide viral load distribution, our concern is not on doses so small that the risks are negligible, but on the high-dose tail instead. If we assume every infected passenger has the moderately large fixed viral load from Miller et al. (2022), no passenger received an airborne dose over 1 PFU, whereas allowing for very high viral loads can result in cases where many passengers received airborne doses over a reasonable estimate of the ID50 (7 PFU) (Fig. 3(a)). This means that viral load is by far the biggest driving factor to infection through airborne doses in a well-mixed air environment, which is consistent with current knowledge that infrequent but significant superspreading events often involve airborne transmission (Cheng et al., 2021; Miller et al., 2021; Zhang et al., 2021).

Conversely, close-range and fomite doses over 7 PFU were more likely with this fixed viral load than with the variable viral load, suggesting a moderately large viral load is more than sufficient for large doses and that a wide viral load distribution dilutes this.

We find that masks can have a major impact in reducing exposure, especially on close-range doses, with a relatively limited impact on fomite doses. This is consistent with other modelling studies, such as Wilson et al. (2021) that show the significant effects of masks on inhalation dose but also an impact on fomite risks. We also find that mask wearing by infected passengers can have a bigger impact than a mask worn by the susceptible as the mask worn by infected passengers reduces all emissions at source, whereas a susceptible passenger wearing a mask would not get protection from potential deposition of large droplets to their eye membranes. Unlike Miller et al. (2022), this paper assumes masks are imperfect with respect to larger droplets (and therefore do not completely remove close-range exposure) and considers a number of mask types. With respect to smaller droplets, we also assume that masks other than FFP2 masks are worn with some gaps.

Our results show that loading and prevalence have a significant impact on the level of exposure. At high prevalence levels, encountering infected passengers is highly likely. However, it is worth noting that this risk is not unique to bus travel, as other settings such as workplaces, schools, shops, and pubs also become riskier during high prevalence periods. While bus encounters are typically short and in reasonably well-ventilated areas, the variability of viral load means there exists a risk of encountering highly infectious individuals, with the risk increasing at high prevalence and loading. Because the aggregated risk of multiple short encounters is still uncertain, we have chosen to assume that doses received during the timescales of a journey may be added together.

Regarding fomite doses and surface contamination, we found that they are widely distributed, and seat choice can greatly affect exposure, especially with traversal poles being highly and frequently contaminated. This is consistent with surface sampling results from Aranega-Bou et al. (2024), where they found traversal poles (they call 'handholds') were among the surfaces most likely to be contaminated with SARS-CoV-2. We treated all mucosal membranes as equal and well-mixed for face touches and have set rules for surface touching when boarding, alighting and seated, such as boarding and alighting had the same distribution of traversal surfaces touched. However, in reality, passengers may touch more traversal surfaces when alighting (when the bus is potentially moving) than when boarding (when the bus is static). We also assumed that passengers do not touch surfaces they bring onto the bus, such as shopping, luggage, or mobile devices. These assumptions may limit the generalisability of our findings.

In this paper, we applied our model to SARS-CoV-2, with assumptions and parameterisation applied accordingly. However, similar assumptions and methodologies could be applied to many other important diseases (especially respiratory) to establish the size of airborne, close-range and fomite doses; in fact, this model was inspired by Lei et al. (2018), where they consider SARS, influenza and norovirus. Different parameterisation will be needed for aspects such as viral load, viral decay rates, hand hygiene efficacy, the RNA to PFU scaling factor and symptoms like coughing frequency. Moreover, the relative importance of these doses, as the contribution of each dose route to the dose-response for different pathogens, will likely differ greatly.

The study results provide important information for policy makers, transport operators and the public travelling by bus. The approach can be used to assess the relative impact of different mitigation measures which enables decision making for both individual exposure risks and the operation of transport services during outbreaks of infectious disease. This may enable different strategies to be taken during different phases of an outbreak, with for example greater emphasis on messaging to wear masks or not travel when sick during higher periods of prevalence. Similarly the results support the need to ensure the travel environment on a bus is well ventilated, informing future vehicle design as well as operating conditions on existing vehicles.

4.1. Strengths and limitations

Our multi-route QMRA approach allows one to assess the role played by each transmission route (close-range, long-range airborne, fomite), as well as the impact of environmental factors, passenger behaviour, and mitigations on exposure. Although our approach in public transport settings is novel in many aspects, such as with respect to incorporating specific passengers' behaviours in these settings, the methodologies described in detail in the Supplementary Material to estimate exposure through each particular transmission route are based on well-established methods in the literature (e.g. fomite contamination equations (King et al., 2020; Wilson et al., 2020); state-space approach to estimate long-range airborne exposure (Parker et al., 2014), or main assumptions around droplet evaporation and deposition (Lei et al., 2018)).

Undoubtedly, this multi-route approach comes with some drawbacks. In particular, some simplifying assumptions need to be made for model tractability, such as the consideration of well-mixed air beyond 2m of the infectious passenger. Alternative approaches to estimate close-range and long-range airborne exposure, such as CFD simulations (Wang et al., 2022; Arpino et al., 2022; Cheng et al., 2022), can be considered instead, which allow one to estimate exposure at an increased spatial resolution. However, the capabilities of those models (in terms of incorporating complex behaviour, running multiple simulations under different conditions, incorporating population heterogeneity or stochasticity) are typically limited due to computational constraints. Alternative approaches such as the Wells-Riley framework have also been considered in this area (Cummings et al., 2024), but they typically only focus on airborne transmission and thus the comparison with other routes (e.g. fomite) is not as clear, and the possibility of differentiating between close-range and long-range exposure is typically more limited.

When comparing to other multi-route QMRA models in the literature (Azimi et al., 2021; Jones, 2020; Lei et al., 2018), although results should in principle be broadly comparable since the underlying techniques are similar, it is important to note that exposure risk is likely to be scenario-dependent. On a bus, individuals share the indoor space for relatively short periods of time, and possibly contact a relatively small set of common surfaces. This is clearly different to a scenario such as the *Diamond Princess* cruise ship outbreak that occurred in early 2020 (Azimi et al., 2021), or interactions in healthcare settings (Jones, 2020). Individuals' behaviours are also likely to significantly depend on the particular setting of study. Moreover, we note that in some studies authors differentiate between doses

received in the lower (LRT) or upper (URT) respiratory tracts, with droplet deposition and fomite transfer typically contributing to URT doses, while aerosol inhalation contributing to LRT doses (e.g. Azimi et al., 2021; Jones, 2020; Lei et al., 2018). Then, a weighted sum can be considered depending on the pathogen of interest, in order to estimate infection risk based on a dose-response approach (e.g. Azimi et al., 2021; Lei et al., 2018). We instead avoided making such assumptions, which can have a significant impact on the model outputs, by focusing instead on predicted exposure through each particular route, rather than estimating infection risk, and thus our results (and in particular the total doses) need to be interpreted accordingly.

Instead of explicitly assessing the probability of infection from a given dose, we report number of doses exceeding 7 PFU. The threshold of 7 PFU was derived from the ID50 (i.e. a dose that infected 50% of individuals) estimate by Killingley et al. (2022), where they used intranasal inoculation in controlled conditions. Although this value carries a great deal of uncertainty, intranasal inoculation is probably closer in nature to the airborne and close doses considered in this paper. It should be noted that vaccination and prior immunity will likely affect the dose required for infection, which is something not explored in this paper. Other studies such as Jones (2020), Wilson et al. (2021) and Azimi et al. (2021) have attempted to estimate infection risk using a dose-response model, however there is considerable uncertainty in this approach as the dose-response is estimated, usually from other coronaviruses (Miller et al. (2022)).

The bus routes we modelled varied in loading patterns and journey timescales, although these loading patterns are idealised and not directly applicable to any particular bus route. In particular, we did not consider a bus taking multiple journeys in the day, where surface contamination might accumulate and spread across the bus during the day. This would more comparable with the end-of-day sampling in Aranega-Bou et al. (2024) and would be a more appropriate timescale when exploring the impact of surface cleaning routines. Additionally, factors not considered here such as passenger demographics, time of day and purpose of travel (e.g. commuting vs. leisure) can influence passenger behavior, such as touching patterns, as well as vulnerability which affects susceptibility to infection and the potential consequences. We also did not account for the possibility of passengers boarding together in groups or families, who may sit together and have similar disease status.

5. Conclusions

Development of a detailed, mechanistic and agent-based QMRA model for a bus environment has allowed the analysis of exposure to SARS-CoV-2 and similar viruses within a bus environment. Assumptions about the viral load distribution were found to have a significant impact on the likelihood of high doses, especially for long-range airborne doses which were found to require significantly higher viral load for passengers to receive a large dose. Prevalence and loading have similar impacts on the probability of receiving a dose and the probability of receiving a high dose, through long-range airborne, close-range airborne and fomites. Masks have no real impact on the probability of receiving a dose but can greatly impact the magnitude of the doses received, especially reducing close-range doses. The model suggests that traversal poles are typically more likely to be contaminated than other surfaces. The choice of seat impacts the close-range and fomite doses received as it impacts how many passengers are in proximity and the number and type of surfaces interacted with. These results are important for considering the relative effectiveness of mitigation measures for policy development, transport operators and individual passengers.

Funding statement

AMB, DM, MFK, KAM, JX, IH, MLG, STP and CJN were supported by the TRACK: Transport Risk Assessment for COVID Knowledge project - EPSRC, EP/V032658/1 -. DM and STP were also supported by the UK Department for Transport.

CRediT authorship contribution statement

Andrew M. Bate: Data curation, Formal analysis, Investigation, Methodology, Software, Validation, Visualization, Writing – original draft, Writing – review & editing. **Daniel Miller:** Formal analysis, Methodology, Software, Validation, Writing – original draft, Writing – review & editing. **Marco-Felipe King:** Methodology, Supervision, Writing – review & editing. **Katy-Anne Moseley:** Writing – original draft, Writing – review & editing. **Jingsi Xu:** Writing – review & editing. **Ian Hall:** Conceptualization, Funding acquisition, Methodology, Writing – review & editing. **Martín López-García:** Conceptualization, Funding acquisition, Methodology, Project administration, Supervision, Writing – original draft, Writing – review & editing. **Simon T. Parker:** Conceptualization, Funding acquisition, Methodology, Project administration, Software, Supervision, Writing – original draft, Writing – review & editing. **Catherine J. Noakes:** Conceptualization, Funding acquisition, Methodology, Project administration, Supervision, Writing – review & editing.

Declaration of competing interest

CJN, STP and IH were participants in the UK Scientific Advisory Group for Emergencies (SAGE) sub-group on environment and modelling which provided guidance on transmission of COVID-19 during the pandemic. The other authors declare that they have no known competing financial interests or personal relationships that could have appeared to influence the work reported in this paper.

Data availability

The data behind figures and tables are available at https://doi.org/10.5281/zenodo.11103471

Acknowledgments

AMB, DM, MFK, KAM, JX, IH, MLG, STP and CJN were supported by the TRACK: Transport Risk Assessment for COVID Knowledge project - EPSRC, EP/V032658/1 -. DM and STP were also supported by the UK Department for Transport. The authors would like to thank the rest of the TRACK team, the EPSRC VIRAL project and UK transport stakeholders on our steering boards for valuable insights as we have carried out this study. The authors thank the Confederation of Passenger Transport (CPT), and UK bus operators within it, for providing estimates on levels of mask wearing on buses during February–March 2022.

Appendix A. Supplementary data

Supplementary data to this article can be found online at https://doi.org/10.1016/j.jth.2024.101829.

References

Aranega-Bou, P., Pottage, T., Fenwick, A., D'Costa, W., Brown, N.F., Yaxley, N., King, M.F., Parker, S.T., Miller, D., López-García, M., Noakes, C.J., Moore, G., Bennett, A., 2024. A 17-month longitudinal surface sampling study carried out on public transport vehicles operating in England during the COVID-19 pandemic identified low levels of SARS-CoV-2 RNA contamination. J. Appl. Microbiol. 135, lxae095.

Arpino, F., Grossi, G., Cortellessa, G., Mikszewski, A., Morawska, L., Buonanno, G., Stabile, L., 2022. Risk of SARS-CoV-2 in a car cabin assessed through 3D CFD simulations. Indoor Air 32, e13012.

Aydin, O., Emon, B., Cheng, S., Hong, L., Chamorro, L.P., Saif, M.T.A., 2020. Performance of fabrics for home-made masks against the spread of COVID-19 through droplets: a quantitative mechanistic study. Extreme Mechanics Letters 40, 100924.

Azimi, P., Keshavarz, Z., Cedeno Laurent, J.G., Stephens, B., Allen, J.G., 2021. Mechanistic Transmission Modeling of COVID-19 on the Diamond Princess Cruise Ship Demonstrates the Importance of Aerosol Transmission, vol. 118. Proceedings of the National Academy of Sciences, e2015482118.

Bandiera, L., Pavar, G., Pisetta, G., Otomo, S., Mangano, E., Seckl, J.R., Digard, P., Molinari, E., Menolascina, F., Viola, I.M., 2020. Face coverings and respiratory tract droplet dispersion. R. Soc. Open Sci. 7, 201663.

Blachere, F.M., Lemons, A.R., Coyle, J.P., Derk, R.C., Lindsley, W.G., Beezhold, D.H., Woodfork, K., Duling, M.G., Boutin, B., Boots, T., Harris, J.R., Nurkiewicz, T., Noti, J.D., 2022. Face mask fit modifications that improve source control performance. Am. J. Infect. Control 50, 133–140.

Caggiano, G., Apollonio, F., Triggiano, F., Diella, G., Stefanizzi, P., Lopuzzo, M., D'Ambrosio, M., Bartolomeo, N., Barbuti, G., Sorrenti, G.T., et al., 2021. SARS-CoV-2 and public transport in Italy. Int. J. Environ. Res. Publ. Health 18, 11415.

Chen, L., Ban, G., Long, E., Kalonji, G., Cheng, Z., Zhang, L., Guo, S., 2021a. Estimation of the SARS-CoV-2 transmission probability in confined traffic space and evaluation of the mitigation strategies. Environ. Sci. Pollut. Control Ser. 28, 42204–42216.

Chen, P.Z., Bobrovitz, N., Premji, Z., Koopmans, M., Fisman, D.N., Gu, F.X., 2021b. Heterogeneity in transmissibility and shedding SARS-CoV-2 via droplets and aerosols. Elife 10, e65774.

Cheng, P., Luo, K., Xiao, S., Yang, H., Hang, J., Ou, C., Cowling, B.J., Yen, H.L., Hui, D.S., Hu, S., et al., 2022. Predominant airborne transmission and insignificant fomite transmission of SARS-CoV-2 in a two-bus COVID-19 outbreak originating from the same pre-symptomatic index case. J. Hazard Mater. 425, 128051.

Cheng, V.C.C., Fung, K.S.C., Siu, G.K.H., Wong, S.C., Cheng, L.S.K., Wong, M.S., Lee, L.K., Chan, W.M., Chau, K.Y., Leung, J.S.L., et al., 2021. Nosocomial outbreak of coronavirus disease 2019 by possible airborne transmission leading to a superspreading event. Clin. Infect. Dis. 73, e1356–e1364.

Cummings, B.E., Haas, C.N., Lo, L.J., Sales, C.M., Fox, J., Waring, M.S., 2024. Airborne disease transmission risks on public transit buses: impacts of ridership, duration, and mechanical filtration using a relative risk metric. Build. Environ. 255, 111303.

Cummings, K.J., Beckman, J., Frederick, M., Harrison, R., Nguyen, A., Snyder, R., Chan, E., Gibb, K., Rodriguez, A., Wong, J., Murray, E.L., Jain, S., Vergara, X., 2022. Disparities in COVID-19 fatalities among working Californians. PLoS One 17, 1–15. https://doi.org/10.1371/journal.pone.0266058.

Dai, H., Zhao, B., 2020. Association of the infection probability of COVID-19 with ventilation rates in confined spaces. In: Building Simulation. Springer, pp. 1321–1327.

Duan, W., Mei, D., Li, J., Liu, Z., Jia, M., Hou, S., et al., 2021. Spatial distribution of exhalation droplets in the bus in different seasons. Aerosol Air Qual. Res. 21, 200478.

Duguid, J.P., 1946. The size and the duration of air-carriage of respiratory droplets and droplet-nuclei. J. Hyg. 44, 471–479.

Goldblatt, P., Morrison, J., 2020. Initial Assessment of London bus Driver Mortality from COVID-19. UCL Institute of Health Equity, London.

Guadalupe, J.J., Rojas, M.I., Pozo, G., Erazo-Garcia, M.P., Vega-Polo, P., Terán-Velástegui, M., Rohwer, F., Torres, M.d.L., 2022. Presence of SARS-CoV-2 RNA on surfaces of public places and a transportation system located in a densely populated urban area in South America. Viruses 14, 19.

Gupta, J.K., Lin, C.H., Chen, Q., 2011. Transport of expiratory droplets in an aircraft cabin. Indoor Air 21, 3–11.

Harbourt, D.E., Haddow, A.D., Piper, A.E., Bloomfield, H., Kearney, B.J., Fetterer, D., Gibson, T., Minogue, T., 2020. Modeling the stability of sever acute respiratory syndrome coronavirus 2 (SARS-CoV-2) on skin, currency, and clothing. PLoS Neglected Trop. Dis. 14 (236), e0008831.

Heinzerling, A., 2022. COVID-19 outbreaks and mortality among public transportation workers—California, January 2020–May 2022. MMWR. Morbidity and mortality weekly report 71.

Ho, C.K., Binns, R., 2021. Modeling and mitigating airborne pathogen risk factors in school buses. Int. Commun. Heat Mass Tran. 129, 105663.

Hu, M., Lin, H., Wang, J., Xu, C., Tatem, A.J., Meng, B., Zhang, X., Liu, Y., Wang, P., Wu, G., et al., 2021. Risk of coronavirus disease 2019 transmission in train passengers: an epidemiological and modeling study. Clin. Infect. Dis. 72, 604–610.

Jones, R.M., 2020. Relative contributions of transmission routes for COVID-19 among healthcare personnel providing patient care. J. Occup. Environ. Hyg. 17, 408–415.

Julian, T.R., Canales, R.A., Leckie, J.O., Boehm, A.B., 2009. A model of exposure to rotavirus from nondietary ingestion iterated by simulated intermittent contacts. Risk Anal.: Int. J. 29, 617–632.

Killingley, B., Mann, A.J., Kalinova, M., Boyers, A., Goonawardane, N., Zhou, J., Lindsell, K., Hare, S.S., Brown, J., Frise, R., Smith, E., Hopkins, C., Noulin, N., Lönst, B., Wilkinson, T., Harden, S., McShane, H., Baillet, M., Gilbert, A., Jacobs, M., Charman, C., Mande, P., Nguyen-Van-Tam, J.S., Semple, M.G., Read, R.C.,

Ferguson, N.M., Openshaw, P.J., Rapeport, G., Barclay, W.S., Catchpole, A.P., Chiu, C., 2022. Safety, tolerability and viral kinetics during SARS-CoV-2 human challenge in young adults. Nat. Med. 28, 1031–1041.
King, M.F., López-García, M., Atedoghu, K.P., Zhang, N., Wilson, A.M., Weterings, M., Hiwar, W., Dancer, S.J., Noakes, C.J., Fletcher, L.A., 2020. Bacterial transfer to fingertips during sequential surface contacts with and without gloves. Indoor Air 30, 993–1004.
King, M.F., Wilson, A.M., Weir, M.H., López-García, M., Proctor, J., Hiwar, W., Khan, A., Fletcher, L.A., Sleigh, P.A., Clifton, I., et al., 2022. Modeling fomite-mediated SARS-CoV-2 exposure through personal protective equipment doffing in a hospital environment. Indoor Air 32, e12938.
de Kreij, R.J., Davies Wykes, M.S., Woodward, H., Linden, P.F., 2022. Modeling disease transmission in a train carriage using a simple 1D-model. Indoor Air 32, e13066.
Lei, H., Li, Y., Xiao, S., Lin, C.H., Norris, S.L., Wei, D., Hu, Z., Ji, S., 2018. Routes of transmission of influenze A H1N1, SARS CoV, and norovirus in air cabin: comparative analyses. Indoor Air 28, 394–403.
Lindsley, W.G., Blachere, F.M., Beezhold, D.H., Law, B.F., Derk, J.M., Hettick, J.M., Woodfork, K., Goldsmith, W.T., Harris, J.R., Duling, M.G., Boutin, B., Nurkiewicz, T., Boots, T., Coyle, J., Noti, J.D., 2021. A comparision of performance metrics for cloth masks as source control devices for simulated cough and exhalation aerosols. Aerosol. Sci. Technol. 55, 1125–1142.
Mathai, V., Das, A., Bailey, J.A., Breuer, K., 2021. Airflows inside passenger cars and implications for airborne disease transmission. Sci. Adv. 7, eabe0166.
Matson, M.J., Yinda, C.K., Seifert, S.N., Bushmaker, T., Fischer, R.J., van Doremalen, N., Lloyd-Smith, J.O., Munster, V.J., 2020. Effect of environmental conditions on SARS-CoV-2 stability in human nasal mucus and sputum. Emerg. Infect. Dis. 26, 2276–2278.
Mbithi, J.N., Springthorpe, V.S., Sattar, S.A., 1993. Comparative in vivo efficiencies of hand-washing agents against Hepatitis A virus (HM-175) and Poliovirus Type 1 (Sabin). Appl. Environ. Microbiol. 59, 3463–3469.
Mei, D., Duan, W., Li, Y., Li, J., Chen, W., 2022. Evaluating risk of SARS-CoV-2 infection of the elderly in the public bus under personalized air supply. Sustain. Cities Soc. 84, 104011.
Mesgarpour, M., Abad, J.M.N., Alizadeh, R., Wongwises, S., Doranehgard, M.H., Ghaderi, S., Karimi, N., 2021. Prediction of the spread of Corona-virus carrying droplets in a bus-A computational based artificial intelligence approach. J. Hazard Mater. 413, 125358.
Miller, D., King, M.F., Nally, J.P., Drodge, J.R., Reeves, G.I., Bate, A.M., Cooper, H., Dalrymple, U., Hall, I., López-García, M., Parker, S.T., Noakes, C.J., 2022. Modelling the factors that influence exposure to SARS-CoV-2 on a subway train carriage. Indoor Air 32, e12976.
Miller, S.L., Nazaroff, W.W., Jimenez, J.L., Boerstra, A., Buonanno, G., Dancer, S.J., Kurnitski, J., Marr, L.C., Morawska, L., Noakes, C., 2021. Transmission of SARS-CoV-2 by inhalation of respiratory aerosol in the Skagit Valley Chorale superspreading event. Indoor Air 31, 314–323.
Moreno, T., Pintó, R.M., Bosch, A., Moreno, N., Alastuey, A., Minguillón, M.C., Anfruns-Estrada, E., Guix, S., Fuentes, C., Buonanno, G., et al., 2021. Tracing surface and airborne SARS-CoV-2 RNA inside public buses and subway trains. Environ. Int. 147, 106326.
Office for National Statistics (UK), 2024. Coronavirus (COVID-19) Infection Survey, UK Statistical Bulletins. https://www.ons.gov.uk/peoplepopulationandcommunity/healthandsocialcare/conditionsanddiseases/bulletins/coronaviruscovid19infectionsurveypilot/previousReleases. (Accessed 22 April 2024).
Ooi, C.C., Suwardi, A., Ou Yang, Z.L., Xu, G., Tan, C.K.I., Daniel, D., Li, H., Ge, Z., Leong, F.Y., Marimuthu, K., et al., 2021. Risk assessment of airborne COVID-19 exposure in social settings. Phys. Fluids 33, 087118.
Ou, C., Hu, S., Luo, K., Yang, H., Hang, J., Cheng, P., Hai, Z., Xiao, S., Qian, H., Xiao, S., Jing, X., Xie, Z., Ling, H., Liu, L., Gao, L., Deng, Q., Cowling, B.J., Li, Y., 2022. Insufficient ventilation led to a probable long-range airborne transmission of SARS-CoV-2 on two buses. Build. Environ. 207, 108414.
Parker, S., Coffey, C., Gravesen, J., Kirkpatrick, J., Ratcliffe, K., Lingard, B., Nally, J., 2014. Contaminant ingress into multizone buildings: an analytical state-space approach. In: Building Simulation. Springer, pp. 57–71.
Pitol, A.K., Julian, T.R., 2021. Community transmission of SARS-CoV-2 by surfaces: risks and risk reduction strategies. Environ. Sci. Technol. Lett. 8, 263–269.
Querol, X., Alastuey, A., Moreno, N., Minguillón, M.C., Moreno, T., Karanasiou, A., Jimenez, J.L., Li, Y., Morguí, J.A., Felisi, J.M., 2022. How can ventilation be improved on public transportation buses? insights from co2 measurements. Environ. Res. 205, 112451.
Ramirez, D.W., Klinkhammer, M.D., Rowland, L.C., 2021. Covid-19 transmission during transportation of 1st to 12th grade students: experience of an independent school in Virginia. J. Sch. Health 91, 678–682.
Sarhan, A.A.R., Naser, P., Naser, J., 2022. Numerical study of when and who will get infected by coronavirus in passenger car. Environ. Sci. Pollut. Control Ser. 1–16.
Schöll, M., Höhn, C., Boucsein, J., Moek, F., Plath, J., an der Heiden, M., Huska, M., Kröger, S., Paraskevopoulou, S., Siffczyk, C., Buchholz, U., Lachmann, R., 2024. Bus riding amplification mechanism for SARS-CoV-2 transmission, Germany, 2021. Emerg. Infect. Dis. 30, 711–720.
Shen, J., Kong, M., Dong, B., Birnkrant, M.J., Zhang, J., 2021. A systematic approach to estimating the effectiveness of multi-scale IAQ strategies for reducing the risk of airborne infection of SARS-CoV-2. Build. Environ. 200, 107926.
Talaat, K., Abuhegazy, M., Mahfoze, O.A., Anderoglu, O., Poroseva, S.V., 2021. Simulation of aerosol transmission on a Boeing 737 airplane with intervention measures for COVID-19 mitigation. Phys. Fluids 33, 033312.
Tomasi, S.E., Ramirez-Cardenas, A., Thiese, M.S., Rinsky, J.L., Chiu, S.K., Luckhaupt, S., Bateman, R., Burrer, S.L., 2021. COVID-19 mortality among amalgamated transit union (ATU) and transport workers union (TWU) workers—march–july 2020, New York city metro area. Am. J. Ind. Med. 64, 723–730. https://onlinelibrary.wiley.com/doi/pdf/10.1002/ajim.23281.
Walker, M.D., Vincent, J.C., Benson, L., Stone, C.A., Harris, G., Ambler, R.E., Watts, P., Slatter, T., López-García, M., King, M.F., et al., 2022. Effect of relative humidity on transfer of aerosol-deposited artificial and human saliva from surfaces to artificial finger-pads. Viruses 14, 1048.
Wang, Q., Gu, J., An, T., 2022. The emission and dynamics of droplets from human expiratory activities and covid-19 transmission in public transport system: a review. Build. Environ., 109224
Wang, Z., Galea, E.R., Grandison, A., Ewer, J., Jia, F., 2021. Inflight transmission of COVID-19 based on experimental aerosol dispersion data. J. Trav. Med. 28, taab023.
Wikipedia, 2024. Wrightbus StreetLite. https://en.wikipedia.org/wiki/Wright_StreetLite. (Accessed 22 April 2024).
Wilson, A.M., Jones, R.M., Lerma, V.L., Abney, S.E., King, M.F., Weir, M.H., Sexton, J.D., Noakes, C.J., Reynolds, K.A., 2021. Respirators, face masks, and their risk reductions via multiple transmission routes for first responders within an ambulance. J. Occup. Environ. Hyg. 18, 345–360.
Wilson, A.M., King, M.F., López-García, M., Weir, M.H., Sexton, J.D., Canales, R.A., Kostov, G.E., Julian, T.R., Noakes, C.J., Reynolds, K.A., 2020. Evaluating a transfer gradient assumption in a fomite-mediated microbial transmission model using an experimental and Bayesian approach. J. R. Soc. Interface 17, 20200121.
Windsor-Shellard, B., Butt, A., 2020. Coronavirus (COVID-19) Related Deaths by Occupation, England and Wales: Deaths Registered between 9 March and 25 May 2020. Office for National Statistics. UK. Online, available: https://www.ons.gov.uk/peoplepopulationandcommunity/healthandsocialcare/causesofdeath/bulletins/coronaviruscovid19relateddeathsbyoccupationenglandandwales/deathsregisteredbetween9marchand25may2020. (Accessed 3 February 2021).
Yang, L., Li, M., Li, X., Tu, J., 2018. The effects of diffuser type on thermal flow and contaminant transport in high-speed train (HST) cabins–a numerical study. Int. J. Vent. 17, 48–62.
Yang, X., Ou, C., Yang, H., Liu, L., Song, T., Kang, M., Lin, H., Hang, J., 2020. Transmission of pathogen-laden expiratory droplets in a coach bus. J. Hazard Mater. 397, 122609.
Yao, F., Liu, X., 2021. The effect of opening window position on aerosol transmission in an enclosed bus under windless environment. Phys. Fluids 33, 123301.
Zhang, L., Li, Y., 2012. Dispersion of coughed droplets in a fully-occupied high-speed rail cabin. Build. Environ. 47, 58–66.
Zhang, N., Chen, X., Jia, W., Jin, T., Xiao, S., Chen, W., Hang, J., Ou, C., Lei, H., Qian, H., et al., 2021. Evidence for lack of transmission by close contact and surface touch in a restaurant outbreak of COVID-19. J. Infect. 83, 207–216.
Zhao, P., Chan, P.T., Gao, Y., Lai, H.W., Zhang, T., Li, Y., 2019. Physical factors that affect microbial transfer during surface touch. Build. Environ. 158, 28–38.